

Numerical modelling and experimental analysis of acoustic emission

S I Gerasimov^{1,2}, T V Sych¹

¹ Siberian Transport University, 191, Dusi Kovalchuk St., Novosibirsk, 630049, Russia

² Tomsk Polytechnic University, 30, Lenina Av., Tomsk, 634050, Russia

E-mail: 912267@gmail.com

Abstract. In the present paper, the authors report on the application of non-destructive acoustic waves technologies to determine the structural integrity of engineering components. In particular, a finite element (FE) system COSMOS/M is used to investigate propagation characteristics of ultrasonic waves in linear, plane and three-dimensional structures without and with geometric concentrators. In addition, the FE results obtained are compared to the analytical and experimental ones. The study illustrates the efficient use of the FE method to model guided wave propagation problems and demonstrates the FE method's potential to solve problems when an analytical solution is not possible due to "complicated" geometry.

1. Introduction

Ultrasound methods are successfully used for testing the elements of the real constructions. However, the scope of such methods is limited by relatively simple elements in geometry. The method of acoustic emission (AE) has fewer limitations related to the size and shape of the object of control; therefore, it is used in testing objects with complex geometry.

In the general case, an acoustic wave contains a set of modes propagating independently of each other through an object of control. The AE sensor registers a superposition of all these modes. Such waves interact with the defects and geometric inhomogeneities, reflecting and refracting on them. The propagation of a wave packet, especially in an inhomogeneous structure, is difficult for analysis in general and for interpretation by the process. One of the possible ways of investigating the propagation of ultrasonic waves is the analytical solution of the corresponding differential equations of motion for the given boundary conditions. This approach is realized for defect-free models with simple geometry [1-3]. However, the analytical solutions become "heavy", i.e. difficult to solve, for the models with complex geometry or for the objects with defects. Another approach to this problem is the numerical solution. There are two basic numerical methods that can be used to solve this problem: the finite element method (FEM) and the boundary element method (BEM). The method of boundary elements has the advantage, which consists in the fact that only the surface of the control object is divided into discrete regions. In fact, the numerical problem becomes one-dimensional.

2. Application of FEM

The equation of motion in the matrix form can be written as:



$$M \cdot \ddot{u} + C \cdot \dot{u} + K \cdot u = F_0, \quad (1)$$

where M is the mass matrix; C is the attenuation matrix (resistance); K is the stiffness matrix; F_0 is the vector of the applied load; u, \dot{u}, \ddot{u} are the displacement vector and its time derivatives.

The spatial and time discretizations are critical for the convergence of numerical results. Integration step Δt ("time increment") is the parameter at which equation (1) has a solution. The choice of such step is important for the accuracy of the solution. The accuracy of the simulation increases with decreasing step Δt . For large Δt steps, the solution in the high-frequency range is obtained with a large error. On the other hand, decreasing the step leads to an increase of the time for solving the problem. It is necessary to search for the optimal value of Δt . For the Newmark integration scheme, this compromise is 20 points for one period of the maximum frequency from a set of propagating waves. This gives an exact solution of equation (1). Such condition can be expressed as:

$$\Delta t = 1/(20f_{max}), \quad (2)$$

where f_{max} is the maximum frequency used.

In the present paper, one-dimensional (linear), the two-dimensional (shell type) and the three-dimensional (volume) finite elements are used. In the case where it is necessary to model geometric concentrators such as holes and cracks, the three-node elements are used. The mass distribution of the elements is considered homogeneous. The size of the elements is chosen so that the propagating wave can be spatially resolved. In [4], it is recommended that more than 10 nodes of the finite element model should be at the wavelength, while in [5] this recommendation is 20 nodes per wavelength. Such recommendations can be expressed as follows:

$$l_e = \lambda_{min}/20 \dots \lambda_{min}/10 \quad (3)$$

where l_e is the characteristic size of the element; λ_{min} is the smallest length of the investigated wave.

Similar to the process of determining step Δt , at first it is necessary to determine the step of discretization of the elements with respect to wavelength λ . To obtain accurate results in studying the attenuation of a wave, the study of the dispersion effect may require a higher level of sampling than (3) [6].

Conditions (2) and (3) show that to solve the problem of propagation of a wave with a high frequency, which has high f_{max} values and a small integration step, it is necessary to have substantial computer resources. For example, for a problem with a frequency of the order of $f_{max} = 2\text{MHz}$ and wavelength $\lambda_{min} = 2\text{ mm}$, integration step $\Delta t = 0.025\ \mu\text{s}$ and element size $l_e = 0.1\text{ mm}$ will be required [7].

3. Numerical results and their discussion

To estimate the stability of the results obtained, first let us consider a problem, simple from the geometric point of view - a rod with a length of 1000 m (Model 1 in Table 1).

Table 1. - Finite element Models.

	Length, $L, \text{ m}$	Width, $H, \text{ m}$	Height, $B, \text{ m}$	Element size, m	Amount of elements	Number of nodes	Type of elements
Model 1, Rod	1000	-	-	2	500	501	TRUSS2D
Model 2, Plate	1	0.5	-	$3 \cdot 10^{-2}$	1360	787	SHELL3T
Model 3, Volume	1	1	1	$5 \cdot 10^{-2}$	8000	9261	SOLID

The mechanical characteristics and velocity C_l of the longitudinal wave propagation for the rod are indicated in Table 2 as Material 1.

Table 2. Material properties of models.

	Elastic modulus E , MPa	Poisson ratio ν	Density ρ , 10^3 kg/m^3
Material 1 (steel), $C_l = 5200 \text{ m/sec}$	$2.1 \cdot 10^5$	0.3	7.7

Velocity C_l of an acoustic wave (longitudinal) is determined by the formula:

$$C_l = \sqrt{\frac{E}{\rho}}, \quad (4)$$

where E is the modulus of elasticity, Pa; ρ is the density of the material, kg/m^3 . For a linear model, only the longitudinal wave is analyzed.

The arrival time of the wave before embedding for Model 1 is determined by the formula:

$$t = \frac{L}{C}. \quad (5)$$

The lower side of the rod, which is modeled by beam 2-node elements of the TRUSS2D type ($l_e = 2 \text{ m}$), has restrictions on the movements along the y axis. Figure 1a shows the direction of the application, the amplitude of external force F at the right end of the rod and the dependence of this force on time.

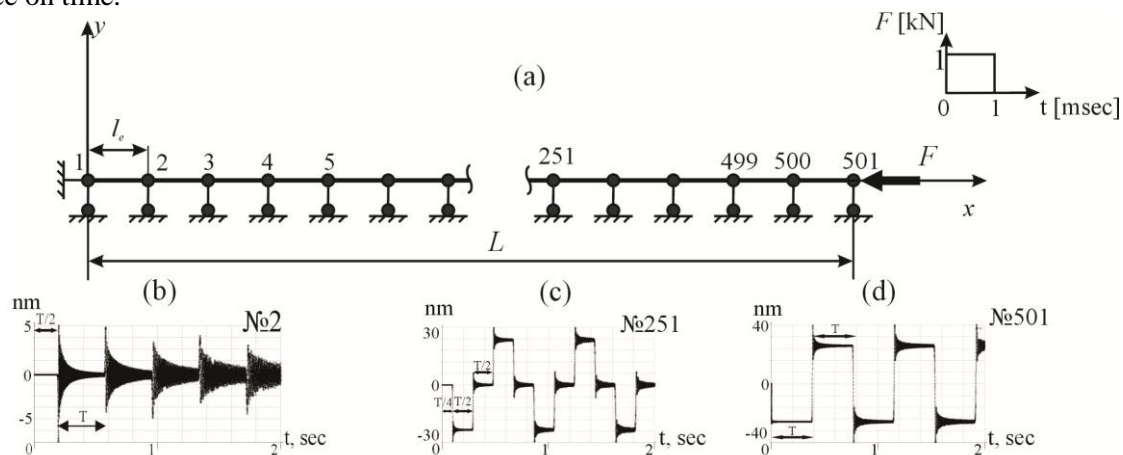


Figure 1. Model 1: (a) - boundary conditions for linear Model 1, (b) - U_x displacement in node 2, (c) - U_x displacement in node 251, (d) - U_x displacement in node 501.

According to the preliminary estimates, the length of the propagating wave from this pulse will be of the order of 6 m, which is comparable to the size of the finite elements of the model. Such applied load corresponds to the excitation of ultrasonic waves with a high frequency. The propagation time of the longitudinal wave along the rod is straight and back (period), $T = 2L/C_l = 0.384 \text{ msec}$. With the help of this model, it is possible to estimate the dispersion effect up to the frequencies of several MHz. In accordance with recommendations (2), the integration step is chosen equal to $\Delta t = 10^{-5} \text{ sec}$. When calculating the transient process, the step is decreased to $\Delta t = 10^{-8} \text{ sec}$.

The different character of U_x displacements is observed in nodes 2, 251, 501 of Model 1, shown in figure 1b, c, d, respectively. It can be seen from figure 1 that the wave in the middle of the rod acquires a complex shape. Near the rigid embedding (figure 1b), the displacement of U_x resembles the damped oscillations of a linear system with greater rigidity. At the free end of the model (figure 1, d), the results of propagation of the direct and reflected waves are seen. For all functions U_x , period $T = 0.384 \text{ msec}$ is strictly repeated.

Let us consider the model of a plane body (Model 2 in Table 1, material 1 in Table 2), shown in figure 3, for different moments of time. On the lower boundary, restrictions on the displacements were introduced, hence $U_y = 0$. The load is applied along both vertical faces in the form of a distributed force (10 N in each node). The pulse shape is shown in figure 3; its duration is 10^{-3} seconds. The characteristic size of the SHELL3T elements is given in Table 1 and is 3 cm, which is ~ 200 times smaller than the wavelength and is consistent with the above-described limitation on the size of the elements. Calculated time step Δt was 100 μ sec for this model. The diameter of the hole is 5 cm. A small finite element mesh is modeled near the geometric concentrator.

Figure 2, a, b shows stress σ_x at times 0.05 msec and 0.15 msec, respectively. The wave propagation front is clearly traced. In Figure 3b wave pulse from both faces reaches the fourth part of the model. Theoretically, the longitudinal wave travels at a known speed and reaches such distance (0.25 m) in the time equal to 0.048 sec (for the fastest mode). Thus, the results of a numerical calculation (figure 2a) coincide with the theoretical (5).

In figure 3b, acoustic waves from the side faces pass $\frac{3}{4}$ of the model around the concentrator. In the middle of the model, the addition of waves occurs, the effect of stress concentration is observed near the hole. Stress concentration factor σ_x is approximately 3, which is in satisfactory agreement with the theoretical solution of the Kirsch problem.

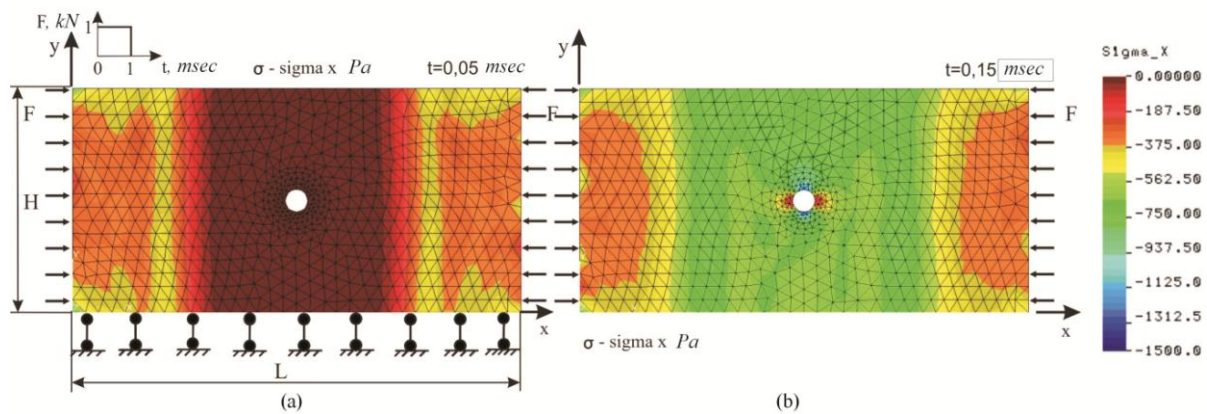


Figure 2. Propagation of a wave pulse in Model 2 (plate): (a) - isolines σ_x through $t = 0.05$ msec after impact; (b) - isolines σ_x through $t = 0.15$ msec after impact.

In [8], an analytical solution was obtained for the problem of the propagation of an acoustic wave in an elastic half-space under the impact of a concentrated force on it. In particular, for longitudinal wave U_l , an expression is obtained for the displacements along acoustic axis z that coincides with the direction of impact:

$$U_l = \frac{F_0 \cdot \Delta S \gamma^2}{2\pi\mu r} \times \frac{\cos \theta (1 - 2\gamma^2 \sin^2 \theta)}{(2\gamma^2 \sin^2 \theta - 1)^2 + 4\gamma^3 \sin^2 \theta \cos \theta \sqrt{1 - \gamma^2 \sin^2 \theta}} e^{-i(\omega t - k_l r)}. \quad (6)$$

where θ is the polar angle of the viewing direction; r is the radius of the observation point; ω is the cyclic frequency of the harmonic oscillation; $k_l = \omega/C_l$ is the wave number; C_l is the velocity of the longitudinal wave; C_t is the velocity of the transverse wave; $\gamma = C_l/C_t$ is the ratio of the velocities.

Distribution U_z obtained from (6) in figure 4b is designated as ANALYTIC. Finite-element Model 3 of a similar problem is shown in figure 3a. Model 3 has the shape of a cube and consists of three-

dimensional elements of the SOLID type. The geometric dimensions and physical properties of it are given in Tables 1 and 2, respectively. Figure 4a shows the model at time 2 msec.

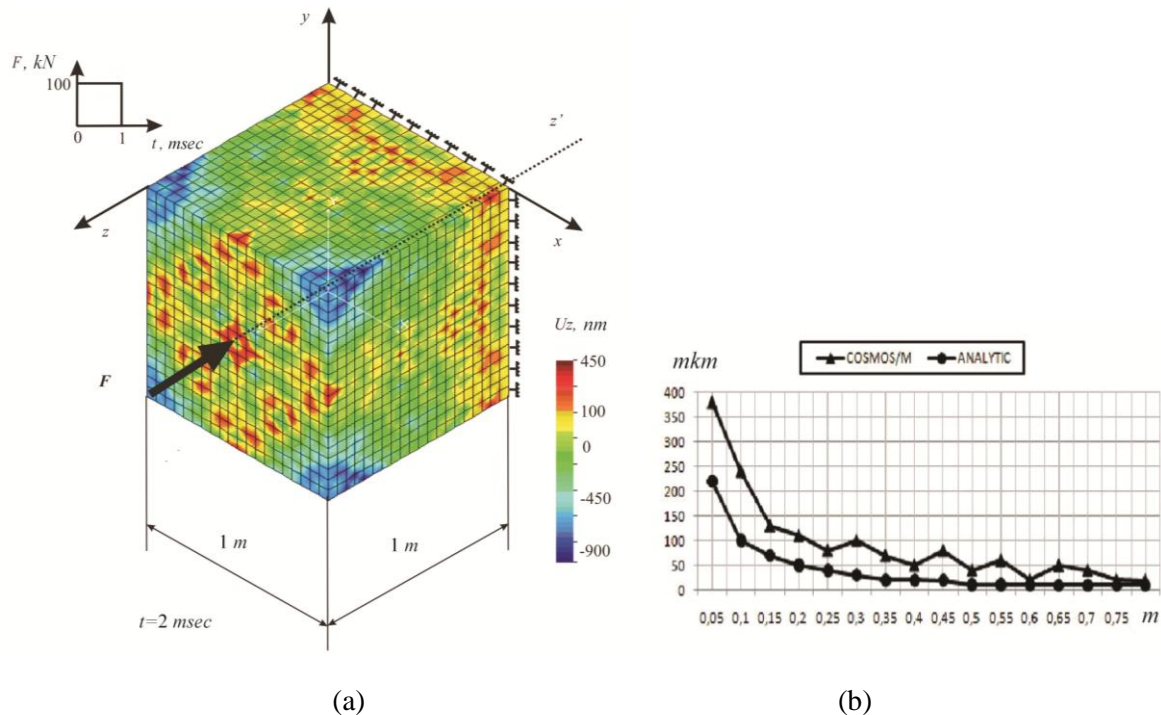


Figure 3. 3D Model 3: (a) - finite element model and boundary conditions; (b) - movements U_z along the acoustic axis.

A force of 100 kN is applied at the central node on the face. The pulse duration is 1 msec. Restrictions on all directions of displacements and rotations are provided along a far face that coincides with axes x , y . In accordance with the recommendations given earlier, the step of time increment was $\sim 5 \cdot 10^{-5}$ sec. The length of the investigated wave is about 6 m. The size of the element was two orders of magnitude lower, which ensures sufficient accuracy of the results obtained.

Figure 3b presents a comparison of the results of theoretical and numerical solutions that qualitatively coincide.

Theoretical calculation of U_z was performed for each node of the finite element model in the direction of the acoustic axis (at $\theta = 0$) (6). The discrepancy of the results to a constant value may be due to errors related to the discretization of the model or to the features of the analytical solution.

4. Hsu-Nielsen's test

The experimental scheme was assembled on vibration-insulated table VIS-1 (Figure 4, a) with a mass of approximately 1000 kg.

The size of investigated plate 2 of material 1 was $0.7 \text{ m} \times 0.4 \text{ m}$. The source of acoustic wave was a brittle fracture of pencil 3 with hardness 2T of 0.3 mm in diameter, pushed out of a colander pencil by 3 mm ($\pm 0.5 \text{ mm}$). Such break (Hsu-Nielsen test) generates an intense acoustic signal, similar to the natural acoustic emission signal [9]. Sensors 4-7 in figure 5, a are sensitive only to displacements U_z of the surface points along the normal to the surface. In a numerical experiment, the requirement for a discretization step in time $1 \cdot 10^{-9} < \Delta t < 5 \cdot 10^{-9}$ sec was fulfilled, as well as for $\lambda = \lambda_{\min} = 0.6 \text{ mm}$, which provided a correct solution of the problem of acoustic wave propagation in a real object.

The finite element model had a rigid fixation along one of the planes, which made it possible to analyze only the high-frequency range. This technique is used to cut off the low frequencies of plate

vibrations. As a rule, acoustic emission signal processing systems operate in the frequency range from hundreds of kHz to tens of MHz.

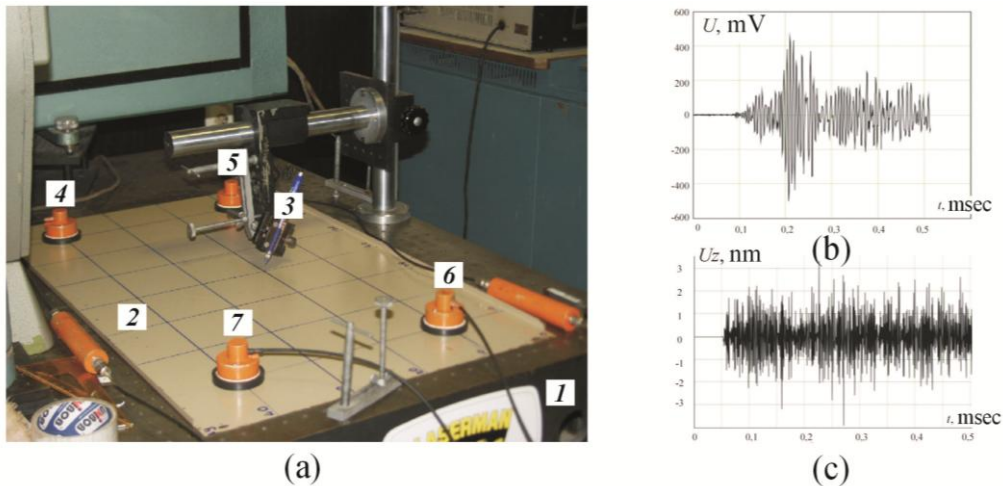


Figure 4. Experimental results: (a) - experimental setup; (b) - response of the 3rd sensor; (c) - numerical calculation results. (1 - vibration-insulated plate, 2 - test plate, 3 - pencil, 4,5,6,7 - sensors for registration of acoustic signals).

This is ensured by the width of the frequency response of the recording sensors themselves and the frequency filtration of signals in the system itself. The load was applied at the site with the same coordinates as the Hsu-Nielsen simulator in the form of a concentrated force (0.5 kN) with a pulse duration of 10^{-7} s. The characteristic size of the SHELL6T elements over the thickness of the plate (which is important in numerical analysis) was 0.6 mm and agreed with above-described calculated value λ_{\min} of the minimum wavelength.

Figure 4b shows the shape of the electrical signal detected by sensor No. 4 of the SCAD-16.03 system [10]. Figure 5c shows the displacement of U_z in the node with coordinates that coincide with the coordinates of sensor No. 4. Comparison of the obtained results allows us to speak about the correctness of the numerical simulation of acoustic signals.

5. Conclusions

The obtained results illustrates the effectiveness of using FEM to simulate the propagation of acoustic waves in linear, planar and three-dimensional objects, when the analytical solution is difficult due to the complex geometry of the models. The influence of two important parameters of FEM - the grid density (the size of the elements) and the step of discretization in time, providing an acceptable accuracy of the solution of the problem - is discussed. The obtained numerical results agree satisfactorily with the analytical and experimental solutions.

References

- [1] Graff K F 1991 *Wave motion in elastic solids* (New York: Dover)
- [2] Builo S I 2004 Diagnostics of deformational and fracture stages based on integral parameters of the flow of acoustic-emission acts *Russian Journal of Nondestructive Testing* **40**(8) 552-560
- [3] Liu G and Qu J 1998 Transient Wave Propagation in a Circular Annulus Subjected To Impulse Excitation on Its Outer Surface *Journal of the Acoustical Society of America* **103**(3) 1210-1220
- [4] Alleyne D and Cawley P 1991 A two-dimensional Fourier transform method for measurement of propagating multimode signals *Journal of the Acoustical Society of America* **89**(3) 1159-1168

- [5] Cleveland R O and Sapozhnikov O A 2005 Modeling elastic wave propagation in kidney stones with application to shock wave lithotripsy *Journal of the Acoustical Society of America* **118**(4) 2667-2676
- [6] Sych T, Gerasimov S, Kuleshov V (2012) Simulation of the propagation of acoustic waves by the finite element method *Russian Journal of Nondestructive Testing* **48**(3) 147-152
- [7] Gerasimov S, Sych T, Kuleshov V (2016) Application of finite elements method for improvement of acoustic emission testing *Journal of Physics: Conference Series* **671** 012017
- [8] Budenkov G A, Nedzvetskaya O V and Dalati M 2003 On Possibilities of Acoustic Remote Nondestructive Testing of Long Objects *Russian Journal of Nondestructive Testing* **39**(11) 833-836
- [9] Hamstad M 2007 Acoustic emission source location in a thick steel plate by Lamb modes *Journal of Acoustic Emission* **25** 194–214
- [10] Ser'eznov A N, Stepanova L N, Kabanov S I, Lebedev E Yu 2002 Microprocessor AE System for Strength Tests of Aircraft Structures *Russian Journal of Nondestructive Testing* **38**(2) 121-126